

Harvard-Smithsonian Center for Astrophysics

Precision Astronomy Group

PROPRIETARY

For FAME Project Team only, competition sensitive.

To:	K.J. Johnston	21 April 1999	TM99-02
From:	J.D. Phillips	30 June 1999	Rev. A ^a
Subject:	FAME single-observation astrometric error.		

Work needed:

- ☐ Thermal analysis and effect on optics.
- ☐ Call Lars Winter.
- ☐ pp. 1-5 need reorganizing.
- ☐ Finish adding 15 m focal length.
- ☐ Summarize largest contributors, and describe what parameters they depend on, which might make them average down, e.g., pixel phase, field position, instrument temperature,
- ☐ Remaining Johnston comments.
- ☐ Remaining Irwin comments..
- ☐ Another meeting with Irwin.
- ☐ More descriptions into text, e.g., II.C.2. Optical distortion, II.C.6. CCD cover plate.
- ☐ Clarify mission accuracy discussion: division of discussion between this memo and Mission accuracy memo.
- ☐ Depth of traps created on-orbit by radiation, and effect of CCD notch, if present.

This memo details the astrometric error affecting single observations by the Full-sky Astrometric Mapping Explorer (FAME)^b [Johnston 98, Johnston 99], and gives derivations. The current release (30 June '99) is still a work in progress, distributed for the purposes of the FAME team as they carry out the current phase A study. Revisions will be necessary, and will continue to be made. Comments are solicited. This version addresses the 15 m focal length design of March 1999. Estimates for the 7.5 m design are given in parentheses.

^a Name changed from "The FAME Error Budget" to "FAME single-observation error". The companion memo "FAME mission accuracy", SAO TM99-05 (Rev. A), has since come out.

^b The design presented in the MIDEX proposal was an evolution of FAME-98 [Reasenberg and Phillips, 1998, Phillips and Reasenberg 1998]. For the MIDEX proposal, the orbit was changed from 100,000 km circular to geosynchronous. In the lower orbit, the solid angle subtended by the Earth is six times larger.

This memo includes <<will include>> substantially lower error estimates for bright stars than those given in the cited proposal and Concept Study Report, obtained by using a different method.

FAME's astrometric accuracy is shown in Table 7, and the systematic error budget is shown in Table 6. Error sources are divided into four parts: I. Stochastic, II. Internal systematic (errors due to the instrument), III. External systematic (errors that would affect an ideal instrument measuring at the same point in space), and IV. Intrinsic (e.g., motion due to resolved companions). Many of the internal errors vary systematically with parameters such as field position and position within the CCD chip. These errors will be well-studied. In a 2½ year mission there will be about 3.8×10^{10} (1.5×10^{11}) faint star observations in total, 2.7×10^9 (1.1×10^{10}) per chip, and 1.3×10^6 (5.3×10^6) per CCD column. Each star is observed 70(270) times by each chip, and 950(3800) times^c by all (faint star) astrometric chips.

Laboratory characterization will determine the nature of the (larger of the) internal systematic errors and support parametric models, particularly of the optics and CCD's. However, before launch, it will not be possible to gather sufficient knowledge for the reduction of the on-orbit observations. In fact, some instrument parameters will change during the mission. Thus, the observations themselves will have to be used to refine the parameters of the pre-launch models. Where necessary, new parameters will be added to model effects that were not discovered on the ground. The vast dataset enumerated above will support the estimation of a large number of instrument parameters, in addition to the astrometric parameters (which will be much more numerous) [Reasenberg 1999b]. Even if it were necessary to include in the model one or more parameters per CCD column, there are sufficient data to support the estimation.

The treatment herein reflects the stages of data reduction. The *a priori* value of a term refers to the uncertainty that can be obtained from using the data of a single observation, as well as any information known independently of FAME (such as spectral type from an independent catalog), and a limited amount of on-orbit modelling (see Appendix A). A *posteriori* refers to the uncertainty that can be obtained by employing all the mission data, astrometric and photometric, as well as ancillary data.

^c This number would increase by 20/14 if the current scheme for bright stars, in which 6 CCD chips have attenuating filters over them, is replaced by one that makes more efficient use of the CCD's, such as a variant of the GAIA scheme in which the clock for a chip with a bright star on it is stopped except for brief intervals in which charge is accumulated, up to the limit imposed by well-filling. The number of medium-bright- and bright-star observations would increase by a factor of 20/3, and 40 times as many photons from bright stars would be detected. While bright stars are relatively few, they are of high scientific interest (almost all of the Cepheids to be observed are bright); also, bright stars contribute importantly to the accuracy of the whole solution, and to determining instrument bias parameters.

Table 1. FAME Parameters. This memo is written with FAME-98 parameters; an update to include the parameters of the 3/99 design is planned for the near future.

Chosen or Specified Parameter	Sym	FAME-98	3/99	Units
Focal length	f	7.5	15	m
Aperture width	S	0.5	0.6	m
Aperture height (each half)	C	0.25	0.25	m
Diffraction width (dist between nulls, unobs.)	$2\lambda_0/S$	0.495	0.413	arcsec
Pixel size	w	15	15	μm
Rotation period	P	20	40	min
Precession rate (Sun-spin plane)	P_p	0.5	0.5	deg./rot'n
Number of pixels, scan	N_s	4096	4096	
Number of pixels, cross-scan	N_c	2048	2048	
CCD read noise	N_r	7	7	e^- rms
CCD QE (assumed independent of λ)				
Optical system throughput				
Field Of View diameter		2.2	1.1	deg.
Derived Parameter	Sym	FAME-98	3/99	Units
Plate scale		0.0275	0.01375	arcsec/ μm
Precession period		10	20	day
Precession of look direction, one rotation to the next, maximum		0.35	0.35	deg
CCD row rate				
Angle subtended by a pixel	θ_{pix}	0.413	0.206	arcsec
Precession-induced smearing (amplitude of sinusoid at rotation frequency)		5.7	5.7	columns

Stellar images move steadily across FAME's focal plane, and the collected charge is shifted in the CCD to follow in Time-Delayed Integration (TDI). Define the scan direction in the focal plane as the direction in which the stars move, and cross-scan as the direction in the focal plane perpendicular to that. FAME has a complex mirror ahead of the primary that causes two fields separated by $\sim 81^\circ$ to create images on the focal plane, one in each half of the pupil, i.e., there are two look directions.

The first component of FAME's error budget is stochastic error. Low stochastic error is a prerequisite for the investigation of other error sources. We have performed numerical experiments to evaluate FAME's centroiding precision (Phillips & Reasenberg 1998). We assumed a blackbody source and modelled the diffraction pattern accordingly, estimating along-scan position, magnitude, and the source temperature. For $V=9$ the precision is 470 (540) μas , and for $V=12.3$ it is TBD (2500) μas . These figures are for $T=5777\text{ K}$; figures for other temperatures are similar. This corresponds to (1/460) of the half-width at null for $V=9$ and (1/100) for $V=12.3$. In the laboratory and using stare mode, centroiding was demonstrated to comparable precision: 1/1200 of the half-width at null with a circular aperture [Winter 1998]. The uncertainties as a fraction of a pixel are (1/770) for FAME ($V=9$) and 1/500 for the laboratory work. FAME uses TDI, which averages some types of error. <<We must find out more, if possible, about Lars' work – the cost to the project is minimal, and the work is relevant. Lars stated to Phillips that he thought the errors he saw in centroiding were due to fitting with the wrong PSF, in particular to failing to model the asymmetry of images due to trailing of images along the CCD column. Winter ascribed this trailing to operating near full-well. His model PSF was obtained by averaging many individual images -- does this yield a good estimator? Norbert Zacharias may know about this work, also.>>

If special provision were not made for bright stars, they would overfill the CCD wells, causing charge to migrate (primarily along the column). The magnitude at which the wells overfill depends on whether the star falls at the center or edge of a pixel, and on the extent to which the observation is smeared laterally due to precession. (The number of columns over which precession spreads the image varies approximately sinusoidally over the 40(20) minute rotation period, with amplitude 5 columns.) The V magnitude at which overfilling occurs is in the range $7 < V < 9$. The accuracy for $V < 9$ is currently calculated assuming that 6 chips are covered with neutral density filters, and bright- and medium-bright-stars are measured only in those chips. One technique, Start-Stop Technology (SST) is under serious consideration for substantially improving the astrometric accuracy in the magnitude range $V < 9$.

There has not been a detailed study of additional error sources using the gated-clock scheme, but here are two, to start the list. 1) Electron traps will delay charge being transferred along a column. Some traps have a timescale comparable with the vertical shift time, so will shift some charge from the leading edge of the image to the trailing. If the TDI happens to stop the image on a trap, it will have time to release its charge. Modelling of the traps is likely to be done by locating individual traps, beginning with a map made in the laboratory. Additional traps will appear due to on-orbit radiation. 2) Other error sources that vary regionally over the CCD will need more detailed models using the gated-clock scheme.

In the remainder of this memo, I discuss the error budget shown in Table 6. The sections below are numbered to correspond to the lines of the table and to the outline of Appendix A.

I. A-B. Statistical Error. The values given here come from the SAO centroiding study [Phillips and Reasenberg, 1998]. When the Modulation Transfer Function (MTF) of the CCD is taken into account, the error values will change somewhat. The MTF of the EEV CCD that FAME plans to use has a full width at half-maximum of 18 μm [Tulloch, 1998], as compared with the pixel size of 15 μm . This MTF is about the smallest obtainable [Geary 1999]. (The sensitivity study at SAO is finished, but not extensively written up. The sensitivity loss is 40-50% in σ , more at 15 m focal length than at 7.5.)

II.A.1. QE Variations. The analysis of bias due to QE variations of SAO TM97-01 applies to a CCD with TDI if the QE variations depend on the applied voltages, and thus move with the stellar image. QE variations that are fixed on the chip will be substantially averaged by TDI, and will be ignored here. QE variations are observed to be largely periodic, and dominated by the lowest-order sinusoidal term << bound higher orders?>>. The measurements to date do not distinguish between variations that are fixed on the chip, and those that move with the charge in

Table 2. Parameters for QE variation.

Parameter	Symbol	Value (FAME-98)
Perturbation amplitude	α	0.05
Pixel angular width	θ_p	0.413 arcsec
Perturbation wavevector	k	15.2 arcsec ⁻¹
Obscuration fractional width	κ	0.4

Table 3. *A priori* uncertainty in fraction of light between 800 and 900 nm, as a function of star temperature. <<This table for 7.5 m focal length>> <<statement on $\sigma(f8)$ >>

T, K	$\sigma(T)$, K	f8	$10^6 df8/dT$, K ⁻¹	$\sigma(f8)$
3000	15	0.378	126.10	0.00187
5777	51	0.191	32.42	0.00165
10000	170	0.122	8.03	0.00136
15000	417	0.097	2.84	0.00119
25000	1208	0.082	0.81	0.00098

TDI. Let the QE be multiplied by a factor $[1 + \alpha \sin(kp + \phi)]$, so that α is the fractional amplitude for the perturbation, k is its wavevector ($2\pi/\text{period}$), ϕ is its phase, and p is angle on the sky in the scan (sensitive) direction. Let f be the number of cycles of perturbation in one diffraction width, $2\lambda_0/S$ (TM97-01, p. 4), where λ_0 is the representative wavelength, 0.6 μm , and S is the aperture width, 0.6 (0.5) m. Let n_s be the number of pixels per diffraction width. For a perturbation whose period is one pixel, $f = n_s$, so $f = 2.0$ (1.2). The fractional width of the obscuration κ is taken here to be 0.5 (0.4), which moderately accurately represents the current design. With these parameters we determine $G(\kappa, f)$ from Fig. 2 of TM97-01 (p. 5). G is -1. This value is exact in the case that an infinite extent of detector is read out. The position bias is

$$\Delta = \Delta_o \cos(\phi) \quad (1)$$

where

$$\Delta_o = \frac{3\alpha}{16\pi(1 - \kappa^3)} \frac{\lambda}{S} G(\kappa, f) \quad (2)$$

(TM97-01, eq. 13). With the parameters given, summarized in Table 2, $\Delta_0 = 400$ (800) microarcsec (μas). The rms variation of Δ over the observations of a star (i.e., ϕ goes from 0 to 2π) is 280 (560) μas .

To determine the level to which this bias can be modelled *a posteriori*, note that stars with $V=9$ have a single-measurement precision of 470 (540) μas . (It is purely coincidence that this precision is nearly the same as the rms value of the bias to be estimated. The value of the bias is unrelated to the accuracy with which it can be modelled, except that a large bias must be proportionately more stable if we are to avoid the need to model its time-variation.) Consider stars with $8.5 < V < 9.5$. Other spans of 1 magnitude will make comparable contributions to the determination of the CCD bias parameters; this advantage is neglected here. Each CCD makes $> \underline{\hspace{1cm}} (3 \times 10^7)$ observations of stars with $8.5 < V < 9.5$. To estimate the above bias to an accuracy of 10 μas using observations with a precision of 540 μas , we need $\sim 800(3000)$ observations. We have four orders more observations than that. The extra observations could be used, if necessary, to model a QE variation that varied with time, or even to model a variation that was different for each CCD column. It seems reasonable that the CCD geometry will be stable with time. Also it is plausible that modelling on a column-by-column basis will not be needed: errors in the printing process used to make the CCD's will tend to vary smoothly from one pixel to the next, perhaps with flaws of a particular type such as the periodic steps in the $\underline{\hspace{1cm}}$ CCD <<Shaklan et al. ref.>>. Clearly, laboratory study of the flight CCD's will be needed, with an emphasis on characterizing the type of defects, for example the periodic steps of Shaklan et al., rather than on measuring them all in the lab to an accuracy sufficient to correct the flight data. A model of the latter scope and accuracy is best derived from the on-orbit observations themselves. A preliminary look at the computation requirements for estimating one parameter per CCD column indicates that it is feasible with current hardware.

II.A.2.b. CCD Wavelength-Dependent Absorption. This effect arises because the optical system is not telecentric, so away from the center of the field, the beam impinges on the detector at an angle. The absorption length in the detector depends on wavelength, and therefore on the object's spectrum.

Let θ_f be the field angle (maximum astrometric field is 1.1°), f be the effective focal length, 15 (7.5) m, and d_p be the distance from the exit pupil to the detector, 370 (97) cm. Then the angle at which the beam impinges on the detector is

$$\theta_1 = \frac{f}{d_p} \theta_f = 2.2 (8.5)^\circ \quad (3)$$

This angle is reduced when the beam enters the silicon. Taking the index to be 3.5 and the thickness 15 μm , the lateral travel for a photon that gets right through is 0.2 (0.8) μm . The photons are detected throughout the thickness. For wavelengths longer than 800 nm, a substantial fraction of the photons go right through. In this wavelength range, the average offset upon detection is half the maximum given above, i.e., 0.1 (0.4) μm or 1 (8) milliarcsec (mas). When averaged over wavelength, the shift depends on the fraction of photons in the band from 800 nm to the long wavelength limit (here taken to be 900 nm), which I call here f_8 .

A priori, the temperature of a V=9 star can be known to an uncertainty $\sigma(T)$ (Table 3) from determination of the apparent width of a single observation. The effect of a non-perpendicular beam depends on f_8 , the fraction of the star's radiation detected by FAME that is in the band from 800 to 900 nm. The effect on temperature is proportional to the derivative of f_8 with respect to temperature. From Table 3, the *a priori* error in f_8 is <0.002 , so the *a priori* angle bias is $<<\text{new number for 15 m will be substantially less than } 55>> \mu\text{as}$. Furthermore, the bias would cancel in the average of the two or three observations of a single passage across the focal plane due to the symmetry of the CCD layout (see below).

A posteriori, the 950(3800) determinations of temperature of the star can be used to improve the temperature estimate, as well as the 270 (1080) photometric observations. The abundance of observations imply that even a variable star's spectrum can be characterized adequately. The expected *a posteriori* angle bias is $<1 \mu\text{as}$.

Symmetry of CCD layout. Several biases depend on field angle. There is a substantial reduction of the effect because of the symmetry with which the detectors are laid out. Consider scan and cross-scan axes in the focal plane (Fig. _). Flipping the up-scan part of the focal plane to down-scan would be a reflection in the cross-scan axis. A star that crosses the focal plane is observed in two or three CCD's, and these are symmetrically laid out in both scan and cross-scan. If asymmetrical CCD layouts are considered, consideration should be made of the systematic error consequences. It must be pointed out that the symmetry should not be relied upon too heavily: some observations will inevitably be asymmetrical due to bad CCD columns, or even the failure of a whole chip.

II.A.2.d. Fringing. The bias due to fringing in the CCD still needs to be accounted for. An error due to fringing in an up-scan chip will be accompanied, to first order, by an equal and opposite error in the down-scan chip. If the star crosses a chip that is on the cross-scan axis, the effect of fringing is cancelled within the chip itself. This cancellation is imperfect if the fringing is different in the two chips, or in the up-scan and down-scan portions of a single centered chip. Differences in the fringing will arise due to variations in CCD thickness and if there are variations in the absorption length.

II.A.3.b. Charge Transfer Effects -- Along-column bleed near full-well. In the laboratory centroiding experiments [Winter 1998], charge transfer effects due to well-filling lead to a bias of approximately 1/500 pixel. Winter says that he did not adjust his PSF for well-filling. Also, his PSF was obtained from an average of many of his standard observations, rather than by adjusting the parameters of a theoretical PSF, or from a PSF measured at higher magnification. This average empirical PSF may have resulted in further biases. Therefore, the 1/500 pixel result should not be interpreted as a universal limit.

A priori. Taking Winter's results at face value, for FAME 1/500 pixel is 400(800) μas . This effect will be largely repeatable, with a component that depends on the phase of the observation with respect to the pixels. The phase of the 950(3800) observations of one star will be uniformly distributed. The bias due to well-filling may however have a component that always tends to retard the star in the scan direction. This systematic component is likely to depend on which

column the observation falls in, and may depend to some extent on the stellar spectrum. If we only require that we model these effects to ~10%, the large number of data available are likely to support the creation of a sufficiently accurate model.

Therefore, the *a posteriori* error will be <<was <80, with 7.5 m focal length>> μas .

II.A.3.d. Charge traps. An effect that will vary from column to column is trapping, which will affect charge transfer, moving collected electrons from the leading edge of the image toward the trailing. Columns with one or more traps will have an additional contribution to the astrometric error. This contribution may depend on temperature, if the trap parameters do. Traps may hold hundreds of electrons, although there are only a few tens of these on each chip [EEV 1999]. Traps created on-orbit by radiation may tend to hold only one or a few electrons. Some traps hold their charge long enough to create a delay in the along-column (2.5 kHz) shift. (A trap that holds its charge very much longer would still be full from the last star that passed along the column, and wouldn't take charge from the current image.) Also, the depth and lifetime can vary with CCD temperature. There will be a varying bias from column to column. I assume here that all the large traps will be known about and modelled, probably prior to launch. Consider, then, traps holding 20 electrons. They are presumably more numerous than the larger traps. If 20 electrons are shifted from the leading edge of a full-well ($V \sim 9$) image (which has 10^5 electrons) to the trailing, the *a priori* shift is $1/5000$ pixel, or $40 \mu\text{as}$, an order less than the single-measurement uncertainty. For a star near the faintest magnitude, say 15, the shift is 10 mas , equal to the single-measurement uncertainty. *A posteriori*, the traps of lesser depth, including those created on-orbit by radiation, can be modelled. The accuracy may be limited because the number of electrons a long-life trap will accept will depend on the recent illumination history (over the last few seconds or minutes) of the trap. <<USNO can make a map of intensity to the required accuracy, which could be used in removing the effect of illumination history!>> Temperature changes of the CCD may also make traps vary. <<how deep are the traps caused by radiation? F. Harris is investigating>> <<Might contamination change a trap?>>. <<We expect to have to estimate parameters for substantially fewer than one trap per column.>>

A trap affecting one column of an image will in general delay the image asymmetrically, which will complicate efforts to detect companions by the widths of the images.

Traps will affect only a proportion of observations of a star. Thus, collecting together all 950(3800) measurements, some will be outliers and can be identified. The column numbers that the outliers went through can be examined for columns likely to contain a trap. Those points can be set aside for later work. That work might include modelling the traps, perhaps using the known density of starlight on the sky to deduce how much charge the trap was able to hold.

II.B.1. Incorrect stellar spectrum model. <<II.B.1. discussion not yet available for 15 m focal length.>> The position of a star symmetrically located with respect to the pixels could be estimated without knowing the width of the image. However, in almost all cases a knowledge of the width, shape, and amplitude of the distribution is essential.

For a solar-type star, our covariance study of centroiding has shown that the temperature of a black body equivalent to a V=9 star at 5777°K can be determined to 1% in a single observation [Phillips and Reasenber, 1998]. Stars that are much hotter have less well-determined temperature, but for those stars, the portion of the spectrum that falls within the FAME passband is similar, so this larger fractional uncertainty in temperature does not indicate large unknown variations in spectrum, so unknown biases in angle. In fact, the covariance study shows that when V magnitude is held constant, the angle uncertainty when fitting stellar temperature is largely unchanging.

With this information about the spectrum, it is reasonable that the position can be determined *a priori* to 1/100 pixel. The mission error on position can be as low as 15 μ as. Here I assume that the temperature can be determined well enough that the error in the spectrum model contributes less than three times this error, i.e., about 50 μ as. <<?? reasoning for this?>>

Work is underway at SAO on fitting real stellar spectra both with appropriate model spectra whose parameters are estimated, and with model spectra that are deliberately inappropriate.

II.B.2. Undetected companions. Companions are detected by FAME with surprisingly high sensitivity by examining the apparent width of the image in all directions, using all data from the mission: separations as small as ~250 μ as <<check Δm range>> can be detected (see below). If undetected, however, a companion causes a shift in the center of light. Two or more objects whose orbital motion over the course of the mission is significant must be reduced as a single multicomponent model in stage VI of data analysis (catalog creation). It may be just possible for companions to be close enough to have significant orbital motion, yet sufficiently separated that the images are separate and would ordinarily generate separate "postage stamps" of detector pixels read out. For example, a binary of separation 10 AU at 10 pc has an apparent separation of 1 arcsec. Its motion would be extremely well-measured, so the small departure from linearity of motion might be significant. <<easy calculation - do it.>>

Detected companions can be modelled, and positions for all stars of the system derived, probably to an accuracy comparable with that obtainable if they were single stars, except for the effect of shot noise from an overlapping image of comparable or greater brightness. <<This is a POINTS result. Do we have substantiation useful in the context of FAME?>> An undetected

Table 4. Uncertainties in a three-parameter fit for angle, magnitude, and temperature. Results are derived from an average of the information matrix over pixel phase. Apparent magnitude has been held constant at V=9 by adjusting bolometric magnitude. The correlation coefficient between magnitude and temperature is c23. (Correlation coefficients between angle and magnitude, and angle and temperature, averaged over pixel phase, are zero to within computational accuracy, as they must be by symmetry.) From SAO covariance study.

Temp, K	$\sigma(\theta)$, μ as	$\sigma(\text{mag})$	$\sigma(T)$, K	c23	m _{bol}
3000	373	14.1	14	-0.9960	7.10
5777	532	2.1	50	-0.4253	8.90
10000	524	21.7	159	0.9958	8.64
15000	485	51.8	379	0.9993	7.85
25000	421	110.8	1076	0.9999	6.40
35000	377	161.7	2030	1.0000	5.27

companion will bias the estimates of position and proper motion, and to a lesser extent, parallax. The shift of the center of light, for a system with the maximum undetected separation, is $\sim 1/4$ of the separation or $60 \mu\text{as}$, and occurs when the magnitude difference is ~ 2.9 .

To detect a companion, we use all estimates for the image width of that object over the entire mission. The width of the image, i.e., effective temperature, can be estimated for a $V=9$ star to within 1% in a single measurement (Phillips & Reasenberg 1998). Since the width is $\sim 300 \text{ mas}$, the single-measurement precision is 3 mas . Roughly half of the $\sim 950(3800)$ measurements can be used to get image widths in two orthogonal directions^d, so the mission precision is $\sim 60 \mu\text{as}$. For systems with separation of the components greater than $\sim 250 \mu\text{as}$ <<arbitrary>>, modeling of the Point Spread Function (PSF) will detect the companion, and positions will be estimated separately for both.

Orbits with period less than $0.8 \times$ the mission duration will also be detected in the position residuals, and longer-period orbits with substantially less sensitivity [Reasenberg, et al., in prep.]. Systems with separation and magnitude such that they escape detection, yet a large enough shift of the center of light to be a significant error source, will constitute a source of error. <<This is 10's or 100's of μas for stars in a quite small volume of parameter space. More work needed.>>

II.B.3. Onboard clock error. *A priori.* A possible clock is the EMXO series of oven-stabilized quartz crystal oscillators made by Vectron Laboratories, Norwalk, CT. <<I think better oscillators are available for a comparable price - \$20-30K. Much better crystal oscillators are available for a much higher price, \$200-300K, from Johns Hopkins University Applied Physics Laboratory. These latter devices have no cost advantage over Rb or Cs masers.>>

Table 5. Ball EMXO clock stability.

τ , sec	root Allan var.	Time root var., sec	Equiv. angular root var., μas
0.1	1×10^{-11}	10^{-12}	0.001
1.0	1×10^{-11}	10^{-11}	0.01
10	5×10^{-12}	5×10^{-11}	0.05
500	$3.5 \times 10^{-11*}$	$1.8 \times 10^{-8*}$	19^*

* Assuming that the Allan variance for $\tau > 10 \text{ sec}$ degrades as $\tau^{1/2}$.

Error in the onboard clock is equivalent to a rotation variation, and can be modelled as such. In principle, the onboard clock might vary rapidly compared with the rotation rate. The EMXO oscillator, however, has the short-term stability given in Table 5, which shows that the variance on long time scales is most important. (The temporal behavior of the EMXO is probably typical for ovenized quartz resonators.)

^d There is nothing magic about two directions: one could take hundreds of directions and build up a crude image in analogy with the tomography in medical imaging.

A posteriori. The clock error over one rotation will be estimated with data from the 10^4 stars with $9 < V < 11$ observed during that rotation. For these observations, the photon-statistics-limited error is 1300 μs . The clock error can therefore be estimated to about 13 μs . This rough estimate is consistent with the more accurate estimate of the uncertainty of estimating rotation parameters [Chandler and Reasenberg, in prep.].

II.C.1. Telescope geometry changes. Lockheed's text in the 8/98 proposal stated that no part of the FAME instrument optics or structure would change temperature from its nominal by more than 5 mK. With a temperature coefficient for low-expansion GrCy of $10^{-7}/\text{K}$, this implies $\sim 100 \mu\text{s}$ error. This is likely to vary smoothly over a rotation, and could in that case be readily removed by modelling. A tilt of an element would appear as a drift in the basic angle, for example, and would affect all $\sim 10^3$ stars of $V < 10$ measured in that rotation. Therefore, geometry changes are likely to be modellable to better than 10 μs .

II.C.2. Optical distortion.

<<JDP to write>>

II.C.6. Refraction in CCD cover plate.

<<JDP to write>>

II.D.1.a. Rotation rate changes – fuel sloshing. For the MIDEEX proposal, a N_2H_4 propellant system has been specified, which raises the possibility of torques due to sloshing. No estimates of these torques are currently available, so this error source is not treated here. Also, no attempt is made here to quantify spurious rotation due to leaking of the fuel through the nozzles, which has been a problem on previous spacecraft with low-thrust requirements <<refs, e.g. to ranging experiments?>> <<From Table 4-11, Sec. 4.3.2.1, of the 6/18/99 CSR, "CG movement of less than a few microns and fuel slug movement dictated by fluid angular momentum and estimated gap volume (200 cm^3)" -- JDP needs more on this in order to write this section>>

II.D.1.b. Rotation rate changes – Solar torque. *A priori.* The Sun acting on an azimuthally symmetric shield causes no torque about the rotation axis. However, small variations in shield reflectivity cause a substantial torque. These are expected to vary slowly over the mission, and to cause a sinusoidal variation in azimuthal angle; thus they are expected to be modellable. The *a priori* effect, however, is large.

First take the solar shield to be flat. Consider a patch of the shield whose reflectivity is smaller than the average by $\Delta R = 0.01$, whose area is $A_{\text{patch}} = 1 \text{ m}^2$, and which is centered $r_{\text{patch}} = 1 \text{ m}$ from the rotation axis,. The Solar radiation pressure on an absorbing surface at 1 AU from the Sun is $Q = 4.54 \times 10^{-6} \text{ kg m}^{-1} \text{ sec}^{-2}$ [Allen, 1976, p. 161]. The spacecraft moment of inertia about the rotation axis is 200 kg m^2 <<Mook, memo of 1998?>>. The force along the (anti-)Sun direction is

$$F_o = Q A_{\text{patch}} \cos(\xi) \Delta R_{\text{patch}} \quad (4)$$

where $\xi = 45^\circ$ is the angle between the Sun direction and the spin axis. The force perpendicular to the spin axis is

$$F = F_o \sin(\xi) . \quad (5)$$

and the torque about the spin axis is

$$\tau = F r_{\text{patch}} \sin(\varphi) \quad (6)$$

where φ is the angle of rotation about the spin axis. The angular acceleration is

$$\alpha = \frac{\tau}{I} = \alpha_o \sin(\varphi) \quad (7)$$

where

$$\alpha_o = \frac{Q A_{\text{patch}} \Delta R_{\text{patch}} r_{\text{patch}}}{I} \cos(\xi) \sin(\xi) . \quad (8)$$

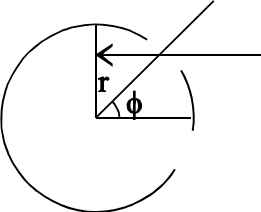
The angular perturbation is

$$\Delta\varphi = \int_{t_o}^t \int_{t_o}^{t'} \alpha_o \sin(2\pi \frac{t''}{P}) dt'' dt' = -\frac{P^2 \alpha_o}{4\pi^2} (1 + \sin x) , \quad (9)$$

where in the second equation, $x = 2\pi t/P$, and t_o has been chosen to be $-P/2$. The rms angular departure from rotation at a constant rate is $P^2 \alpha_o / (4\sqrt{2} \pi^2)$, which is 0.6 arcsec for the parameters given above. The *a priori* bias is almost five orders of magnitude larger than the permissible *a posteriori* bias.

Since the effect of a single patch (of arbitrary size) on a *flat* shield is to cause a purely sinusoidal angular perturbation at the rotation frequency, the effect of all such reflectivity variations will also be a single sinusoid at the rotation frequency, with only two parameters to be determined: amplitude and phase. There are other effects that can cause other types of perturbation. If the shield is conical instead of flat, for example, the projected area of the above patch will vary over the rotation, and the perturbation will no longer be sinusoidal.

A posteriori. A variation in rotation is much like a variation in onboard clock frequency, discussed above. The variation due to solar radiation pressure on a flat shield has two parameters, the amplitude and phase of the angular perturbation. (There would be small additional effects, resulting in additional parameters to be determined, if the shield and solar power array are not quite flat.) The discussion of clock error above shows that a single parameter, the rotation rate, can be estimated to $\sim 13 \mu\text{s}$ from the data of a single rotation. There were 10^4 data used for this estimate. Because the number of data is large, a substantial number of additional <<sufficiently non-degenerate>> parameters can be estimated to comparable accuracy, with little degradation in the accuracy of the science parameters. <<We now have VIRGO data on solar variability, and Murison is calculating the effect on spacecraft attitude in-scan as well as cross-scan.>>

II.D.1.c. Rotation due to Earth light shining in the ports. *A priori.* The Earth is less bright than the Sun, but shines directly into the view ports during a portion of each rotation at two epochs per orbit. The flux emitted by the Earth is $F_E = 340 \text{ watt/m}^2$. At the MIDEK altitude of 35786 km, the geometric coupling factor $\ll\text{define}\gg$ is 0.023. Take the port area to be $A_p = 0.2 \text{ m}^2$ (larger than the actual beam at the aperture to allow for beam clearance). Assume that the port lies at 45° to the radiation, which is the angle at which torque is likely to be maximized, depending on the geometry of the surface the light happens to strike inside the instrument. The power coming in is 1.1 watt. This power exerts a force of 4×10^{-9} newton, which acts at a radius of $\sim 1 \text{ m}$, at an angle ϕ (Fig. ) of $\sim 60^\circ$, creating an angular acceleration of $2 \mu\text{as/sec}^2$. Supposing that this acceleration has a duration of 45° of rotation, it causes a perturbation of 20 mas. This perturbation will be difficult to predict well, since it depends on which structures within the spacecraft are struck by the Earth radiation, which may vary somewhat from rotation to rotation. Its overall amplitude also depends on the weather on Earth, and on the fraction of the side exposed to the spacecraft which is sunlit.

A posteriori. Observations will be used to model this effect to an accuracy comparable to that for the solar torque, but depending on how well it is possible to fit data from several adjacent rotations with a single model, it may require a significant increase in the number of parameters to be determined.

II.E. Imperfectly-determined grid. There had been no data reduction errors *per se*, as they are things like centroiding with the wrong model of the PSF or spectrum, and are included under other error budget items.

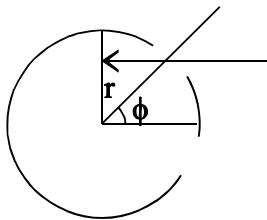


Figure 1. Earth light and port geometry.

February 21, 1999: I have put in reduction errors in the spiral and global stages, but are these any more than *a posteriori* reflections of the perturbations such as Earthlight shining in the ports? For starters, what drives the errors John sees in his study? I think it's no more than the Gaussian errors on the stellar observations. If correlations create larger errors in the spiral and global models than one would calculate via $\text{root}(N)$, I think they deserve a position in the error budget.

III.A. Ephemeris.

To correct for stellar aberration, the spacecraft velocity must be known. A velocity error of 1 cm/sec causes a $7 \mu\text{as}$ error in the aberration correction. The spacecraft velocity $\ll\text{??}\gg$ would vary on the timescale of the orbital period, 1 day $\ll\text{??}\gg$ so that the bias due to velocity error would be the same for $\ll\text{how many??}\gg$ observations, and could be estimated to $50 \mu\text{as}/\sqrt{\text{??}} = \ll\text{??}\gg$.

Table 6. Error Budget - Single Measurement

§	Source	Error (microarcsec) [1]		Averaging characteristics
		<i>a priori</i>	<i>a post- eriori</i>	
I.A.	Photon Statistics			
I.A.	• V=9	540	540	
I.A.	• V=15	10800	10800	
I.B.	• Read noise, 7 e - rms, V=15	6600	6600	
II.A.1	QE Variation	560	<10	
II.A. 2.b.	CCD Wavelength- Dependent Absorption	300	30	Varies with field & wavelength
II.A.3.	Charge Transfer Effects	800	80	Varies with column number
II.B.1.	Incorrect Stellar Spectrum Model	4000	50	Periodic in pixel phase
II.B.3	Onboard Clock Error	<10	<1	
II.C.1.	Telescope Geometry Changes	100	<10	
II.C.2	Optical Distortion	2000	20	Varies with field position
II.C.6.	Refraction in CCD Cover Plate	1	<1	
II.D.1.	Rotation Rate Changes	10 ⁶ [2]	<1	
III.A.	Ephemeris (1 cm/sec knowledge)	7	<1	

General notes for Table 6.

(1) *A priori* and *a posteriori* refer to the error before and after modeling (fitting) using iterative astrometric data reductions. The *a posteriori* errors are dominated by photon statistics, and all will be largely uncorrelated from one epoch to another. To arrive at the values in [Table 1], the photon statistics plus residual errors are divided by the square root of the number of measurements, with a small quantity added in quadrature (10 microarcsec) to account for correlations.

(2) Due primarily to Solar radiation pressure on the shield, whose reflectivity varies spatially (we assume 1% over 1 m²). The rotation error varies smoothly over a rotation, and changes very little from one rotation to the next. Therefore, it can be modeled to very high accuracy. Somewhat more difficult to model is the rotation error due to Earth radiation (reflected and reradiated) entering the viewports, which causes a rotation variation of order 20 mas, but the torque varies according to which instrument structures are illuminated, and the weather on Earth. Data from a single rotation suffice to model the spacecraft attitude to the level shown.

Appendix A. FAME error budget, outline form

Note that Fringing has recently moved from II.A.1.f to II.A.2.d.

I. Statistical error

- A. Photon statistics, $V=12.3$, position: single-measurement (mission), $\mu\text{as} \dots 2400$ (50)
- B. Read noise & dark current. 7 e^- rms raises the variance a factor two for a star of $V=15$.

II. Internal systematic error.

A. CCD Errors.

- 1. QE variations.
 - a. Intra-pixel variations that move with accumulating charge.
 - b. Inter-pixel.
 - c. Wavelength-dependent.
 - d. Non-linearity.
 - e. Bad pixels & columns.
- 2. Detection of photons in the wrong pixel.
 - a. Fixed on chip.
 - b. Beam non-perpendicular, with wavelength variation of absorption.
 - c. Dependence of Modulation Transfer Function (MTF) on wavelength.
 - d. Fringing (in red).
- 3. Charge transfer effects.
 - a. Efficiency (CTE) in the wake of a bright star.
 - b. Along-column bleed when approaching full-well.
 - c. Deterioration due to radiation damage.
 - d. Charge traps.
- 4. Electronics. Roundoff error?
- 5. Physical flatness.
- 6. Recovery from saturation.

B. Centroiding.

- 1. Incorrect stellar spectrum model.
 - a. Error in estimation of spectral type.
 - b. Metallicity effects.
 - c. Reddening.
 - d. Non-stellar objects.
- 2. Onboard clock error 0

C. Optics.

- 1. Distortion
 - a. Element shape, spacing, and orientation changes, including changes in the basic angle.
 - (1) Thermal
 - (a) differential image motion
 - (b) Common mode image motion
 - (2) Long-term drift, e.g., water loss

2. Gain variation between columns with a skewed PSF changes emphasis on advanced portion of the wing of the image. 0
3. Need to determine the PSF.
 - a. Variation with field, wavelength, time.
4. Non-uniformity of mirror reflectivity varies with time (and PSF is not symmetrical.) 0
5. Temperature difference in CCD cover, combined with dn/dT .
6. Contamination of CCD or its cover.
7. Cosmic rays.
8. Scattered light.
9. Ghost images.

D. Rotation.

1. Spin rate changes.
 - a. Viscosity of station-keeping fuel slows the rotation.
 - b. Patch on the solar shield has different reflectivity.
 - c. Earthlight shining in ports - variable torque.
 - d. Motion of heat pipe working fluid, if one is used (currently, one will not be).
 - e. Thermal expansion of spacecraft.
 - (1) Consider radiator plates, e.g., 3 looking out the sides, seeing the Earth.
 - f. Nutation damper stiction (the damper must be linear down to very small displacements).
 - g. Solar radiation variations
 - h. Solar wind.
2. Error in axis direction – star doesn't go directly down columns
 - a. Confusion.
 - b. Read noise (faint limit).

E. Imperfectly-determined "grid".

1. Rotation spiral model errors. (This has no *a priori* component.)
2. Global model errors. (This has no *a priori* component.)

III. External systematic error.

- A. Ephemeris. 0

IV. Intrinsic error, or signal.

- A. Detected companions.
 1. Resolved.
 2. Unresolved.
- B. Undetected companions.
- C. Stellar activity.

Appendix A. Models included and effects accounted for in *a priori* centroids. (Ergo, these effects do not increase the error. Errors in these models do, however.)

Quantity modelled	Yields
Optical element powers and spacings, as-designed	Lowest-order model of distortion
On-orbit focal length estimate (enough parameters to model structural drift vs. time to adequate accuracy)	First correction to above
Spacecraft rotation (12 parameters per rotation)	Rotation model to account for rotation rate, and perturbations thereto (e.g., dark patch on solar shield and solar variability) and clock error.
Stellar temperature	
Depth and location (column and row numbers) of traps holding >20 e	Bias due to those traps (including variation of effect with subdivision of the column in SST)

References

Geary 1999.

Geary, J, SAO, priv. communication 1999.

Johnston 1998.

Johnston, K.J. "Full-Sky Astrometric Mapping Explorer (FAME)", Proposal to NASA's Explorer Program, Medium-Class Explorers (MIDEX) and Missions of Opportunity, Aug. 18, 1998.

Johnston 1999

Johnston, K.J., "Full-Sky Astrometric Mapping Explorer (FAME)", Phase A Concept Study Report for NASA's Explorer Program, Medium-Class Explorers (MIDEX) and Missions of Opportunity, June 18, 1999.

Phillips 1998.

Phillips, J.D., and R.D. Reasenberg, "Optical System for an Astrometric Survey from Space", Proc. of Conference 3356 on Space Telescopes and Instruments V, Kona, HI, SPIE (1998).

Reasenberg 1998.

Reasenberg, R.D., and J.D. Phillips, "Design of a Spaceborne Astrometric Survey Instrument", Proc. of Conference 3356 on Space Telescopes and Instruments V, Kona, HI, SPIE (1998).

Reasenberg 1999a.

Reasenberg, R.D., R.W. Babcock, and J.D. Phillips, "An Astrometric Planet Search, Simulations and Mission Characteristics", in preparation, 1999.

Reasenberg 1999b.

Reasenberg, R.D., "FAME Parameter List", 4/21/99, on FAME web site:
http://aa.usno.navy.mil/FAME/internal/TechCommittees/DataModeling_params.pdf

Tulloch, 1998.

Tulloch, S., RGO Technical Note 118, "The Measurement of Spatial Resolution in EEV4280 CCD Images", 7 July, 1998.

Winter 1998.

Winter, L., private communication, 1998. Based on work towards a thesis at the Hamburg Observatory. <<W. van Altena will try to ask Winter or C. DeVegt about this work when in Germany 3/4/99, ..., especially to see if there is something written that we may cite, or at least read.>>

Distribution

R. Reasenberg

I. Shapiro

FAME Web page *via* M. Murison and S. Horner